Progress In Electromagnetics Research C, Vol. 70, 123–133, 2016

Design of Short-Length Polarization Beam Splitter Based on Highly Birefringent Dual-Core Photonic Crystal Fiber

Zhenpeng Wang[1, *], Fei Yu[1, 2], Zhuo Wang[2], and Huimin Liu[3]

Abstract—We propose an all circular-air-hole short-length polarization beam splitter (PBS) with high extinction ratio based on dual-core highly birefringent photonic crystal fiber (PCF). The impacts of geometrical parameters on the coupling polarization dependence, coupling length ratio (CLR), and propagation property are numerically investigated by the full-vector finite element method (FEM) and the semi-vector beam propagation method (BPM). From simulation results, it is seen that CLRs at the excitation wavelength of 1.55 µm can be optimized to be closed to the desired values of 3/2 and 4/3 to satisfy the sufficient condition of splitting polarized modes by appropriately tailoring the air-hole sizes. For the two optimal structures, the separation of x- and y-polarized modes can be achieved in short lengths of 1.41 mm and 2.89 mm at the operating wavelength of 1.55 µm, respectively. Furthermore, the extinction ratios at $\lambda = 1.55\,\mu$m are estimated to be 97.7 dB and 88.1 dB, and the wavelength bandwidths of extinction ratio better than 15 dB are about 107 and 82 nm, respectively.

1. INTRODUCTION

PBS, which can separate TM and TE polarization modes, is an important passive optical device, and it is widely used in optical fiber communication systems as well as fiber optical sensing systems [1]. In the literature, various configurations of integrated optic PBS based on branched waveguides have been presented, where highly birefringent materials, such as $L_iN_bO_3$ or compound semiconductors, were employed [2, 3]. Since the technology for fabrication of PBS in these materials is relatively complex, interest has emerged in the fabrication of these devices in glass waveguides and optical fibers [4]. However, one major disadvantage of conventional fiber PBS is that a long coupler length is required because of the small birefringence in conventional glass fibers [5, 6]. In recent years, PCFs have attracted great attentions for their unique flexibly controllable properties, such as endlessly single mode, high birefringence, controllable chromatic dispersion, and high nonlinear property [7–10]. Since the experimental fabrication of twin-core PCF was reported in Refs. [11, 12] and confirmed the possibility of using the PCF as an optical fiber coupler [13], different geometrical configurations of PBSs based on dual- or multi-core PCFs have been intensively presented [14–18]. Compared to conventional fiber-based PBSs, PCF-based PBSs can achieve short length and high extinction ratio, and PCFs have the advantage of that they are much easier to make into multiple cores and/or more complex structures [19].

From the view point of the device configuration, PCF-based PBSs can be classified into two types [20]. The first type of PBS possesses an asymmetric configuration, in which only the selective polarized mode can be freely coupled between PCF cores while the other polarized mode is intentionally entrapped into the incident core [21–23]. Although broad bandwidth can be realized in this type of PBS, it shows a low extinction ratio due to the fact that modal coupling cannot be prohibited completely.

Received 20 November 2016, Accepted 19 December 2016, Scheduled 5 January 2017

* Corresponding author: Zhenpeng Wang (wzpdoctor@hrbeu.edu.cn).

[1] College of Automation, Harbin Engineering University, No. 145 Nantong Street, Harbin 150001, China. [2] College of Electrical Engineering and Automation, Harbin Institute of Technology, No. 92 West Dazhi Street, Harbin 150001, China. [3] College of Mechanical and Electrical Engineering, Qingdao Agricultural University, No. 700 Changcheng Road, Qingdao 266109, China.

Besides, in order to select the desired coupling mode by the index-match method, the geometrical constructions are always very complicated to the current fabrication technique. The second type of PBSs is based on symmetric identical twin-core PCFs, relying on the high birefringence to produce a large difference of coupling lengths between x- and y-polarized modes [24–30]. Zhang and Yang [14] firstly reported the symmetric dual-core PCF-based PBS, and showed that the splitting ratio better than -11 dB and a bandwidth of 40 nm could be achieved in a 1.7 mm length. Florous et al. [24] proposed a 15.4 mm-long symmetric PCF beam splitter with uniform elliptically-shaped air holes. Lu et al. [25, 26] realized an ultra-broadband PBS by introducing two fluorine-doped cores with the device length of more than 80 mm. Recently, Jiang et al. [27] designed an circular-elliptic hybrid air-hole PBS with the ultra-short length of 119.1 μm, in which the high extinction ratio of 118.7 dB at $\lambda = 1.55$ μm and broad bandwidth of 249 nm could be achieved. Liu et al. [28] reported a square-lattice Z_nT_e glass PBS with the length of 1.1452 mm. Wang et al. [29] realized an octagonal-lattice PCF-based PBS, whose bandwidth of extinction ratio as low as -15 dB is 82 nm. Wang et al. [30] lately designed a square-lattice circular-elliptical air-hole PBS, and the extinction ratio lower than 20 dB is about 70 nm with the length of 93.3 μm. Although these PCF-based PBS can achieve good performance, their structures are too complex to be fabricated. For example, it is impossible to realize two different kinds of air holes (circular and elliptical) in PCFs using present fabrication techniques [31], and the fabrication of octagonal-lattice PCF remains a challenge to our knowledge. Currently, designing the PCF-based PBS with a simple air-hole pattern is a key issue to make them practical.

In this paper, we propose a novel dual-core PCF-based PBS, characterized by a short length, easy fabrication technology, as well as high extinction ratio. Considering the feasibility of fabrication, the hexagonal lattice (or triangular lattice) and all circular air holes are adopted in the proposed PBS. To optimize the performance, we apply the full-vector FEM to accurately investigate the influence of geometrical parameters on CLR, and then the semi-vector BPM is employed to visualize the light propagation behaviour in longitudinally varying PCF. The simulated results show that the value of CLR at the wavelength of 1.55 μm can be successfully optimized to be 3/2 and 4/3 to meet the sufficient condition of splitting polarized modes. The propagation analysis indicates the separation of x- and y-polarized modes can be achieved in short lengths of 1.41 mm and 2.89 mm at $\lambda = 1.55$ μm. Finally, the corresponding extinction ratios and wavelength bandwidths are also discussed. From the point of fabrication, the proposed PCF-based PBS possess the advantage that the shape of all air holes are uniformly circular and arranged in the triangular lattice that is easy to fabricate with the method of stack and draw.

2. THEORETICAL MODEL

According to the normal-mode coupled theory, the coupling of a dual-core fiber can be described by the use of the supermodes [32, 33]. When light is incident into one core, the propagation mode of the core is excited. An exponentially decaying portion of mode field will diffuse into the cladding and inevitably enter the other core due to the small distance between two cores. Then this energy may be trapped in the other core and becomes a source for a propagating mode. Then the propagating modes in two cores will couple each other. Therefore, there are four polarization components in the dual-core structure, and can be denoted as E_x^{even}, E_y^{even}, E_x^{odd}, and E_y^{odd}, where the superscripts of even and odd represent the even and odd modes, and the subscripts of x and y are the x- and y-polarized modes. The x and y components of the electric field along z direction can be described by the overlap of even and odd modes for x- and y-polarized modes [33]:

$$\begin{aligned}\overrightarrow{E_x}(x,y,z) &= a_+\overrightarrow{E_x^{even}}(x,y)\,e^{in_x^{even}kz} + a_-\overrightarrow{E_x^{odd}}(x,y)\,e^{in_x^{odd}kz}\\ \overrightarrow{E_y}(x,y,z) &= a_+\overrightarrow{E_y^{even}}(x,y)\,e^{in_y^{even}kz} + a_-\overrightarrow{E_y^{odd}}(x,y)\,e^{in_y^{odd}kz}\end{aligned} \tag{1}$$

where a_+ and a_- are the excited coefficients of even and odd modes, and they satisfy the condition of $0 < a_+, a_- < 1, a_+^2 + a_-^2 = 1$. k is the wave number. $n_{x,y}^{even}$ and $n_{x,y}^{odd}$ denote the effective refractive indexes of the even and odd modes for x- and y-polarized modes, respectively. The phase difference between even and odd modes for two orthogonal polarized modes can be obtained by

$$\delta_{x,y} = kz\left(n_{x,y}^{even} - n_{x,y}^{odd}\right) \tag{2}$$

From Eq. (2), we can see that the value of $\delta_{x,y}$ varies with the propagation distance. When the variation value of the phase difference is π, the corresponding propagation distance is defined as the coupling length, which can be used to quantify the strength of coupling. The coupling length for x- and y-polarized modes at the wavelength of λ can be derived from Equation (2):

$$L_i = \frac{\pi}{\left|\beta_i^{even} - \beta_i^{odd}\right|} = \frac{\lambda}{2\left|n_i^{even} - n_i^{odd}\right|} \tag{3}$$

where $i = x$, y, β_i^{even} and β_i^{odd} are the propagation constants of even and odd modes for the i polarization, respectively. The coupling lengths of x- and y-polarized modes are different due to the high birefringence in this splitter, i.e., a complete power transfer for x polarization and y polarization happen at different lengths. In order to successfully separate two polarization modes, the total physical length L of the device are required to satisfies the sufficient condition $L = mL_x = nL_y$ where m and n are positive integers with opposite parity. Therefore, we define the coupling length ratio (CLR) as:

$$CLR = \frac{L_y}{L_x} = \frac{m}{n} \tag{4}$$

From the above equations, we can learn that the key of designing a PBS is to obtain an appropriate value of CLR by accurately tailoring the geometrical parameters. The coupling mechanism of the splitter is the beating of the even and odd modes along the coupling region of the proposed structure. If it is assumed that input power $P_{in} = P_{in}^x + P_{in}^y$ is launched into core A, the output powers at the through and coupled ports are given by:

$$\begin{aligned} P_{out}^A &= P_{in}^x \cos^2\left(\frac{\pi L}{2L_x}\right) + P_{in}^y \cos^2\left(\frac{\pi L}{2L_y}\right) \\ P_{out}^B &= P_{in}^x \sin^2\left(\frac{\pi L}{2L_x}\right) + P_{in}^y \sin^2\left(\frac{\pi L}{2L_y}\right) \end{aligned} \tag{5}$$

where P_{in}^x and P_{in}^y denote the input powers of x- and y-polarized modes, respectively, and L represents the propagation distance along the PBS. The extinction ratio (ER) evaluates the performance of the polarization splitters quantitatively and can be defined as:

$$ER = 10\lg\left(\frac{P_{out}^x}{P_{out}^y}\right) \tag{6}$$

Due to the two-fold symmetry of the PBS structure, ERs at through and coupled output ports are the same. So only the through output port is used to evaluate the performance of the proposed PBS.

In addition, numerical simulations play an important role for the design and modeling of PCFs. So far, various theoretical models on analysis of PCFs have been developed, such as effective index approach, plane wave method, BPM, multi-pole method, and FEM [34]. Compared with other methods, the full vector FEM with curvilinear hybrid edge/nodal elements is capable of accurately dealing with the curved boundaries of air holes in PCFs [35], and it has been widely used in the study of PCF properties, including modal birefringence, chromatic dispersion, confinement loss, as well as the coupling property [25–30]. In the simulation, we firstly use the full-vector FEM to accurately investigate its basic characteristics and optimize the value of CLR, and then employ semi-vector BPM to analyze the propagation behaviour and extinction ratio for the optimum structure.

3. GEOMETRICAL STRUCTURE AND SIMULATION RESULTS

3.1. Geometrical Structure and Basic Characteristics

The cross section of the proposed dual-core PBS is shown in Fig. 1, where all the circular air holes are arranged into a hexagonal array. In the transversal profile, symbols Λ and d represent the lattice constant and the diameter of the cladding air holes, and d_1, d_2 and d_3 denote the corresponding diameters of air holes surrounding around the PCF cores, respectively. The refractive index of air holes is assumed to be 1.0, and the background index of silica can be obtained by Sellmeier formula. The two identical cores, A and B, are formed by combination of the small and large air holes and are individually separated by

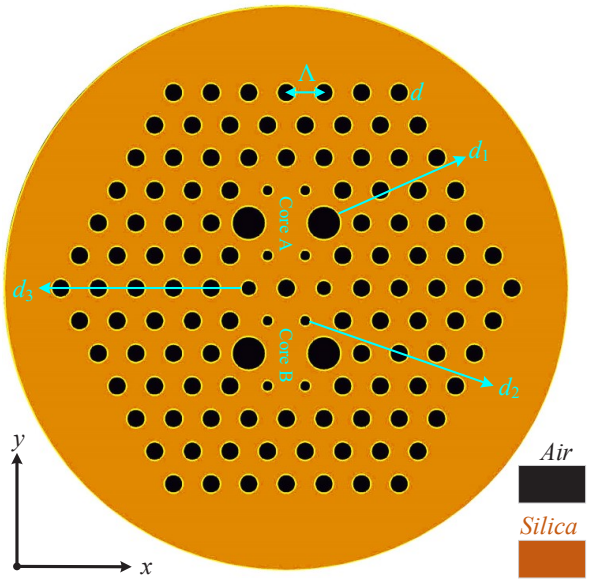

Figure 1. Cross section of the proposed PCF-based PBS.

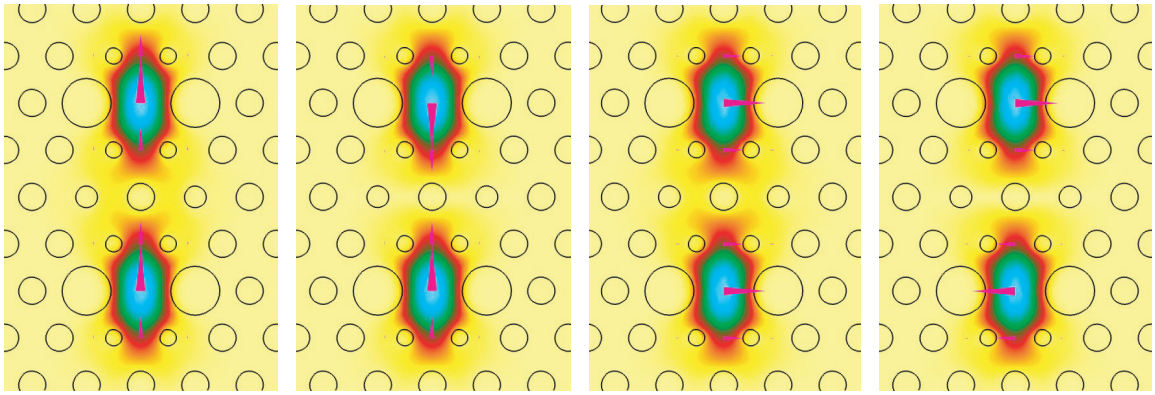

Figure 2. Transverse electric-field distributions at $\lambda = 1.55\,\mu m$. (a) y-polarized even mode, (b) y-polarized odd mode and (c) x-polarized even mode, (d) x-polarized odd mode with $\Lambda = 2.0\,\mu m$, $d = 0.5\Lambda$, $d_1 = 0.9\Lambda$, $d_2 = 0.3\Lambda$ and $d_3 = 0.4\Lambda$.

the central hexagon element. The separated distance between the centers of A and B is $2\sqrt{3}\Lambda\,\mu m$. In each core, two enlarged air holes d_1 are deliberately introduced for enhancing the coupling polarization dependence, and the smaller air holes with the diameters of d_2 and d_3 are designed for controlling the silica bridge of the energy transfer between dual cores so as to ensure a strong coupling.

During the simulation, we firstly evaluate the field distributions of even and odd supermodes at the wavelength of $1.55\,\mu m$ with $\Lambda = 2.0\,\mu m$, $d = 0.5\Lambda$, $d_1 = 0.9\Lambda$, $d_2 = 0.3\Lambda$ and $d_3 = 0.4\Lambda$, as shown in Fig. 2. It can be obviously seen that the field powers are well restricted in the core region although little field power diffuses into the lattice near the core, and the electric field directions in dual-cores are identical for even supermodes but opposite for odd supermodes. Then, the effective refractive indexes of supermodes as a function of wavelength are calculated and illustrated in Fig. 3, where we can find that for the i polarization the effective index n_i^{even} is greater than n_i^{odd} in the whole wavelength range. Moreover, it can be also clearly found that the index difference $\Delta n = n_i^{even} - n_i^{odd}$ increases with the increase of the wavelength, which will lead to the decrease of coupling length according to Equation (3). Fig. 4

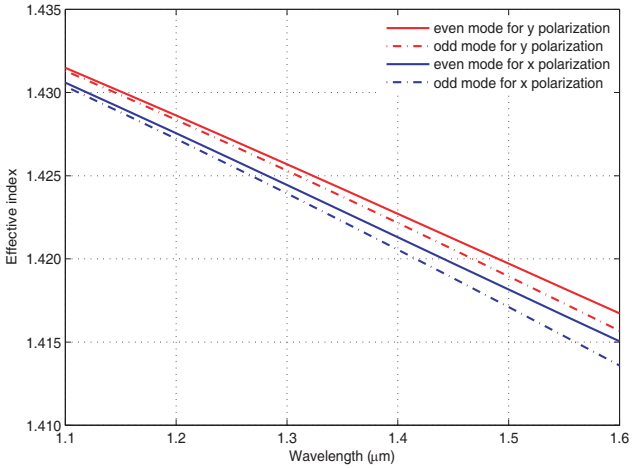

Figure 3. Effective refractive indexes of supermodes for x- and y-polarized modes at different operating wavelengths when the structure parameters are set as $\Lambda = 2\,\mu\text{m}$, $d = 0.5\Lambda$, $d_1 = 0.9\Lambda$, $d_2 = 0.3\Lambda$, and $d_3 = 0.4\Lambda$.

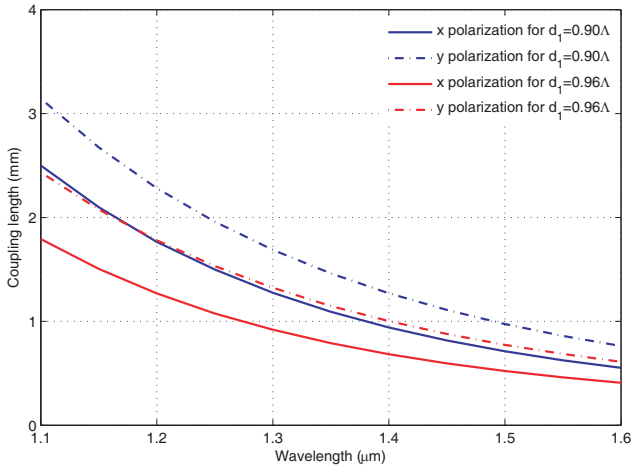

Figure 4. Coupling lengths of x- and y-polarized modes as a function of wavelength with $d_1 = 0.9\Lambda$, 0.96Λ when the structure parameters are set as $\Lambda = 2\,\mu\text{m}$, $d = 0.5\Lambda$ and $d_2 = 0.3\Lambda$, and $d_3 = 0.4\Lambda$.

plots the variation of coupling lengths for two polarized modes at different transmission wavelengths with $d_1 = 0.9$ and 0.96. Firstly, it is apparent that the two polarized modes have different coupling lengths by reason of the highly birefringent core, and this coupling polarization-dependent property plays an critical role in achieving the aim of splitting them. Secondly, the coupling lengths of two polarized modes become apparently shortened when d_1 varies from 0.9Λ to 0.96Λ, because the coupling coefficients of two polarized modes and the birefringence are increased significantly. In addition, at the operating wavelength of $1.55\,\mu\text{m}$ the coupling length is shorter than 0.5 mm, which provides the possibility for realizing the PBS in a several millimeter length.

3.2. Coupling Length Ratio and Parameter Optimization

From Equations (2) and (3), we learn that the total physical length of the splitter relates not only to the coupling lengths (L_x and L_y) but also to their ratio L_y/L_x (CLR). Therefore, it is necessary to investigate the dependent relationship between CLR and geometrical parameters at $\lambda = 1.55\,\mu\text{m}$. From a theoretical point of view, the optimal value of CLR is 2/1. However, although many attempts have been made, CLR fails to be close to the optimal value of 2/1 at $\lambda = 1.55\,\mu\text{m}$. Fig. 5 indicates the impacts of the normalized diameter d_3/Λ on CLR under different situations of d_1/Λ varying from 0.86 to 1.0 with the step of 0.02. The other structural parameters Λ, d and d_2 are fixed to be $2\,\mu\text{m}$, 0.5Λ and 0.3Λ, respectively. It can be clearly seen that the value of CLR obviously increases as d_1 increases for a given fixed d_3, which is mainly attributed to the fact that the birefringence becomes stronger and enhances the polarization dependence. Fig. 5 also illustrates that the value of CLR decreases with the increasing value of d_3 for a given d_1. Most importantly, the desirable values of 3/2 and 4/3 are able to be obtained when the structural parameter group (d_3/Λ, d_1/Λ) are designed appropriately. In addition, it should be noted that there are multiple sets of combinations of (d_3/Λ, d_1/Λ) for CLR = 3/2 and 4/3.

For further optimizing geometrical parameters, the dependence of the variation of parameter d_3/Λ on the coupling length at $\lambda = 1.55\,\mu\text{m}$ is investigated for different values of d_1/Λ with $\Lambda = 2\,\mu\text{m}$, $d = 0.5\Lambda$, and $d_2 = 0.3\Lambda$, as shown in Fig. 6. It is apparent that the coupling length increases with the increase of d_3, because the increase of d_3/Λ makes the silica channel of energy transfer narrower. In the following discussion, we only focus on two cases of CLR that are close to 3/2 and 4/3 for a short-length PBS. According to Figs. 5 and 6, the corresponding parameter group (d_1/Λ, d_3/Λ) is designed to be (0.98, 0.32) for CLR $\approx$ 3/2 and (0.88, 0.31) for CLR $\approx$ 4/3, respectively. For the two optimal PBS structures, the coupling lengths of x- and y-polarized modes are calculated. For the case

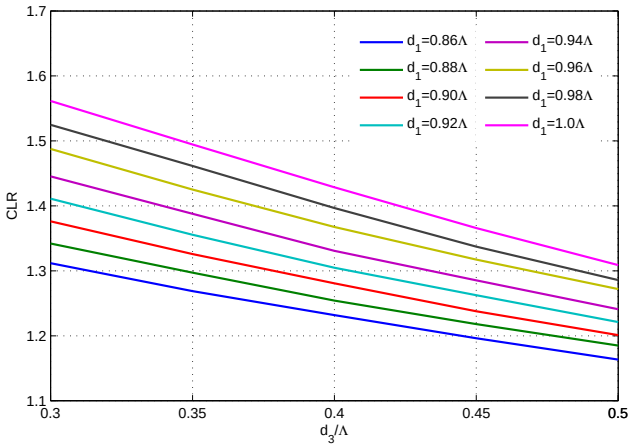

Figure 5. Coupling length ratio CLR as a function of the normalized d_3/Λ for different normalized diameters d_1/Λ at $\lambda = 1.55\,\mu\text{m}$ with $\Lambda = 2\,\mu\text{m}$, $d = 0.5\Lambda$, and $d_2 = 0.3\Lambda$.

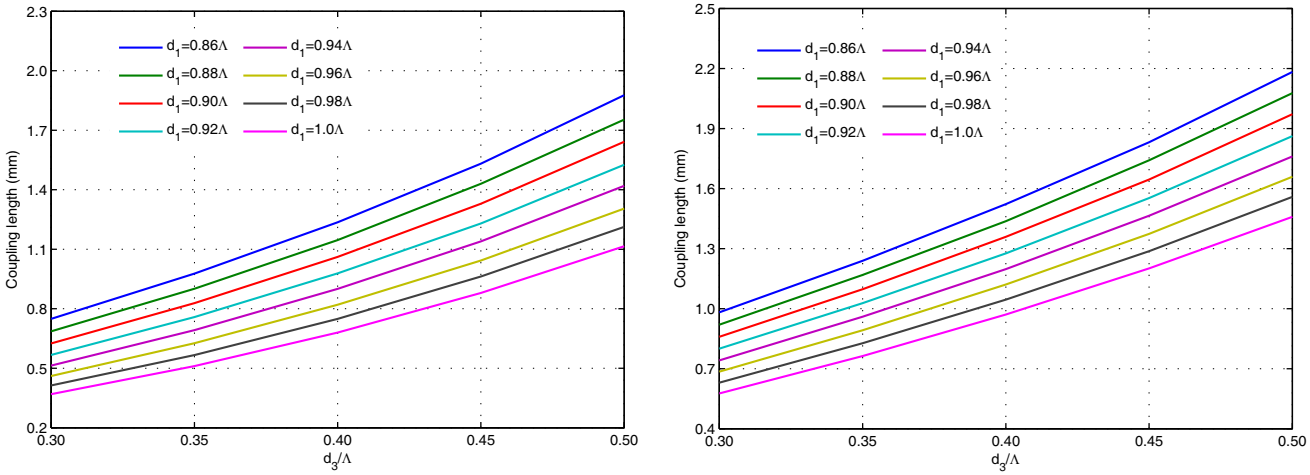

Figure 6. Coupling lengths of (a) x-polarized mode and (b) y-polarized mode as a function of the normalized parameter d_3/Λ for different values of d_1/Λ at $\lambda = 1.55\,\mu\text{m}$ with $\Lambda = 2\,\mu\text{m}$, $d = 0.5\Lambda$, and $d_2 = 0.3\Lambda$.

of CLR $\approx 2/3$, the coupling lengths are about $L_x = 0.471\,\text{mm}$ and $L_y = 0.706\,\text{mm}$, and thus the total length is about 1.41 mm by $L \approx 3L_x \approx 2L_y$; for the other case of CLR $\approx 4/3$ the coupling lengths are respectively $L_x = 0.722\,\text{mm}$ and $L_y = 0.963\,\text{mm}$, so the total length can be obtained about 2.89 mm by $L \approx 4L_x \approx 3L_y$.

3.3. Propagation Characteristics

To visualize the coupling mechanism of the proposed PCF-based splitter, the three-dimensional semi-vector BPM is also employed to model the optimized PBS structures. In the simulation, it is assumed that a given polarization light of 1.55 μm is incident into core A, and then powers in core A and core B will periodically change with the propagation distance. In Fig. 7, we plot the electric field distributions of x-polarized mode at the propagation distance of $z = 0$, $L_x/3$, $L_x/2$, $2L_x/3$ and L_x for the case of CLR $= 3/2$ with the optimal structure of $\Lambda = 2\,\mu\text{m}$, $d = 0.5\Lambda$, $d_1 = 0.98\Lambda$, $d_2 = 0.3\Lambda$, and $d_3 = 0.32\Lambda$. As can be seen in Fig. 7, at the transmission distance of $L_x/3$, only a small portion of the energy couples

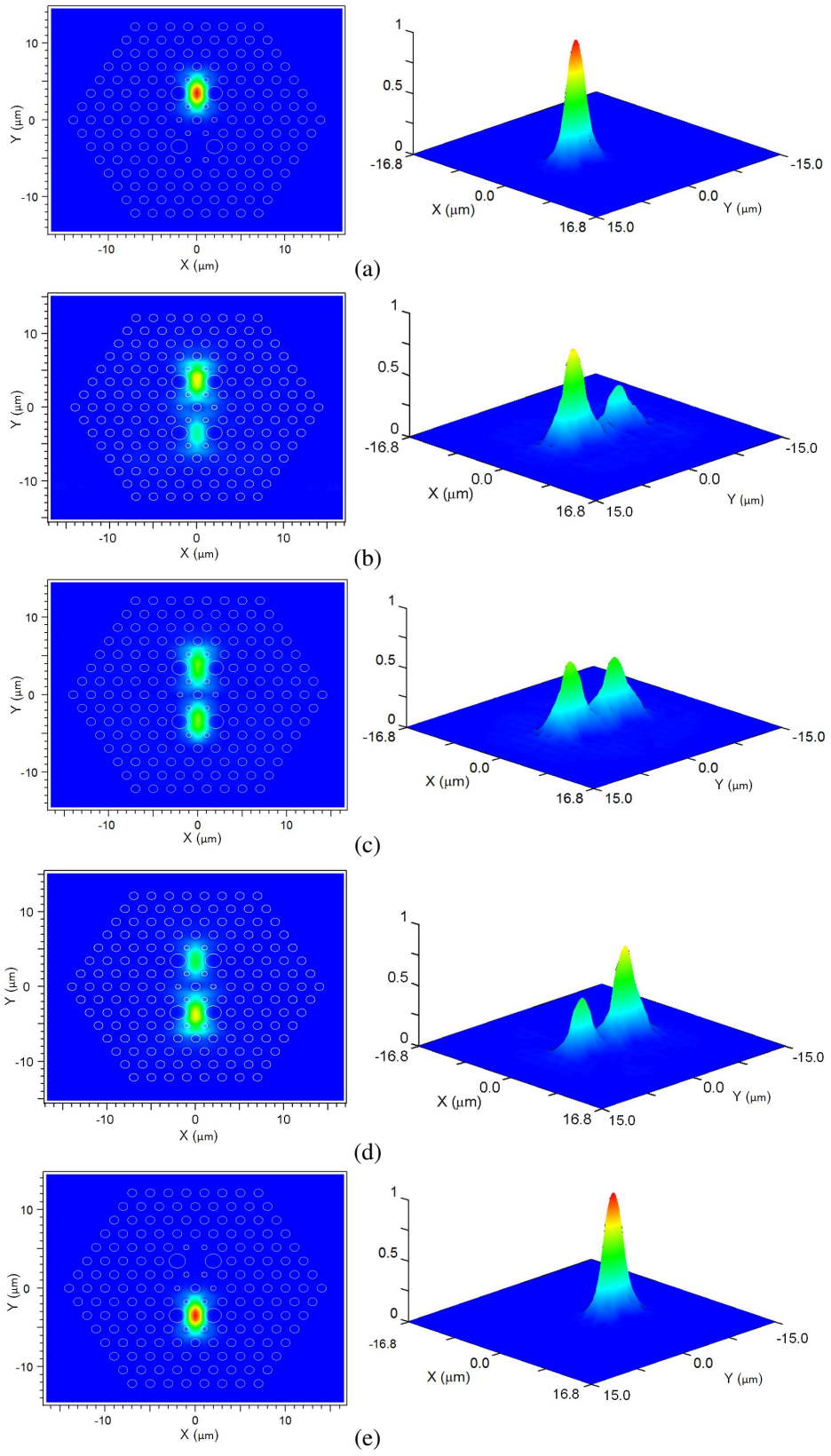

Figure 7. Field distributions of x-polarized mode at the propagation distance of (a) $z = 0$, (b) $z = L_x/3$, (c) $z = L_x/2$, (d) $z = 2L_x/3$, and (e) $z = L_x$.

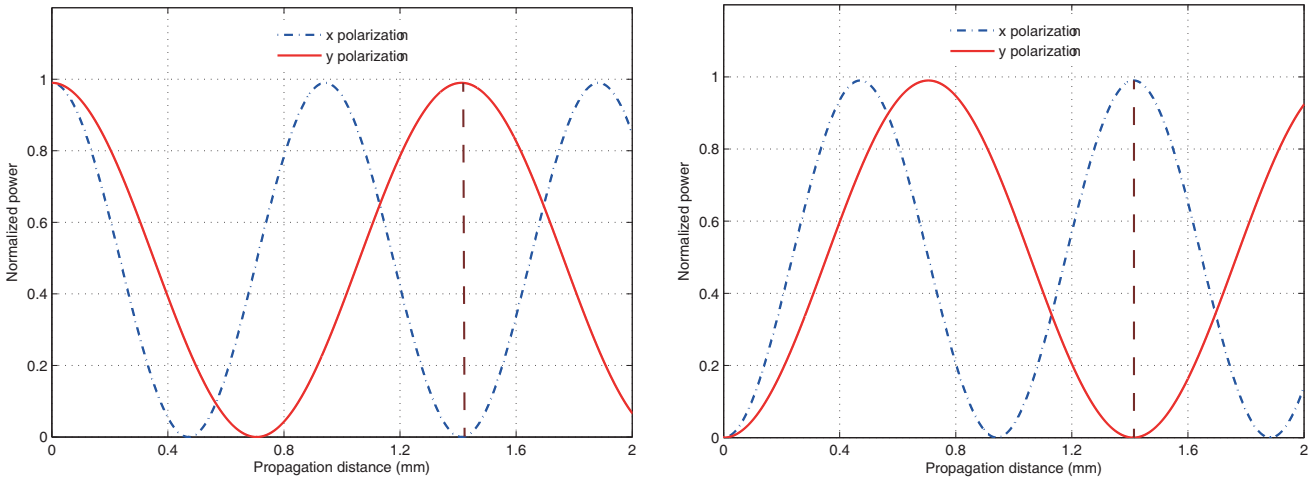

Figure 8. Normalized power of x- and y-polarized modes versus the propagation distance at $\lambda = 1.55\,\mu\text{m}$ in (a) core A, and (b) core B for the case of CLR = 3/2.

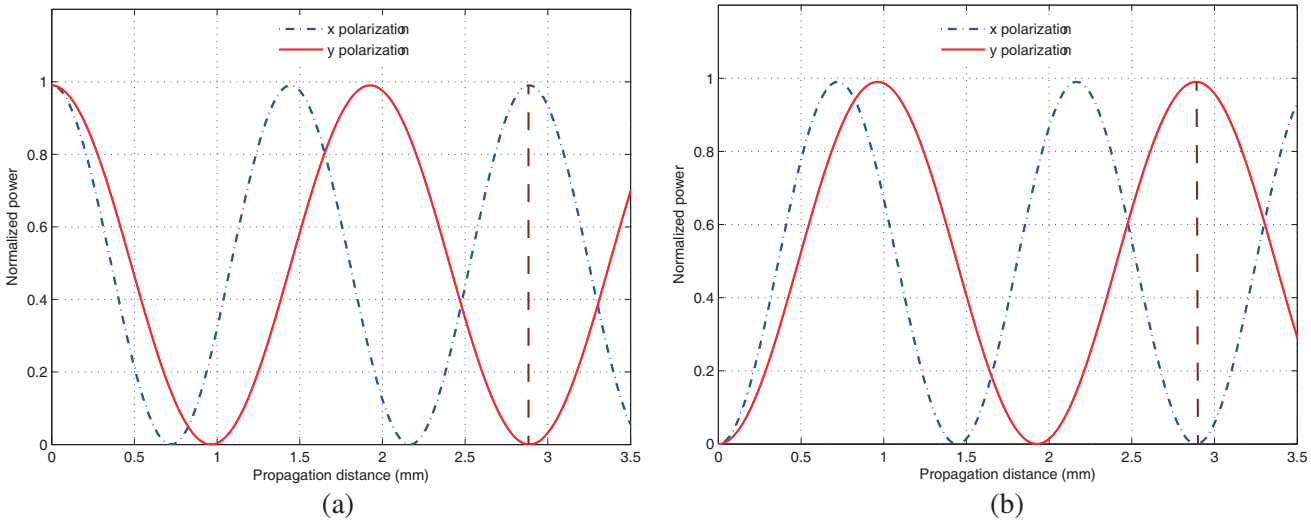

Figure 9. Normalized power of x- and y-polarized modes versus the propagation distance at $\lambda = 1.55\,\mu\text{m}$ in (a) core A, and (b) core B for the case of CLR = 4/3.

into core B from core A, and with the increase of the propagation distance more energy transfers to core B, and till $z = L_x/2$ the powers in dual cores are almost the same. Finally, when the transmission distance reaches the coupling length of L_x, almost all the original power in core A couples into core B. The y-polarized mode also has a similar behaviour to this. Figs. 8 and 9 illustrate the normalized powers in core A and core B against the propagation distance for the two optimal structures. It can be seen that the incident light transfers back and forth between the twin cores, and at the distance of L_x or L_y the power of x- or y- polarized mode in core A almost disappears while that in core B reaches the peak. More importantly, after a propagation distance of 1.41 mm in Fig. 8, almost all x-polarized power stays in the through channel A while that of the y-polarized mode exists in the coupled channel B. Similarly, as Fig. 9 shows, the two polarized modes are also completely divided and couple out from different channels at the distance of 2.89 mm.

The extinction ratio gives the performance of the device to isolate the two polarized lights. Fig. 10 indicates the extinction ratio as a function of wavelength for the two optimal structures. It can be learned

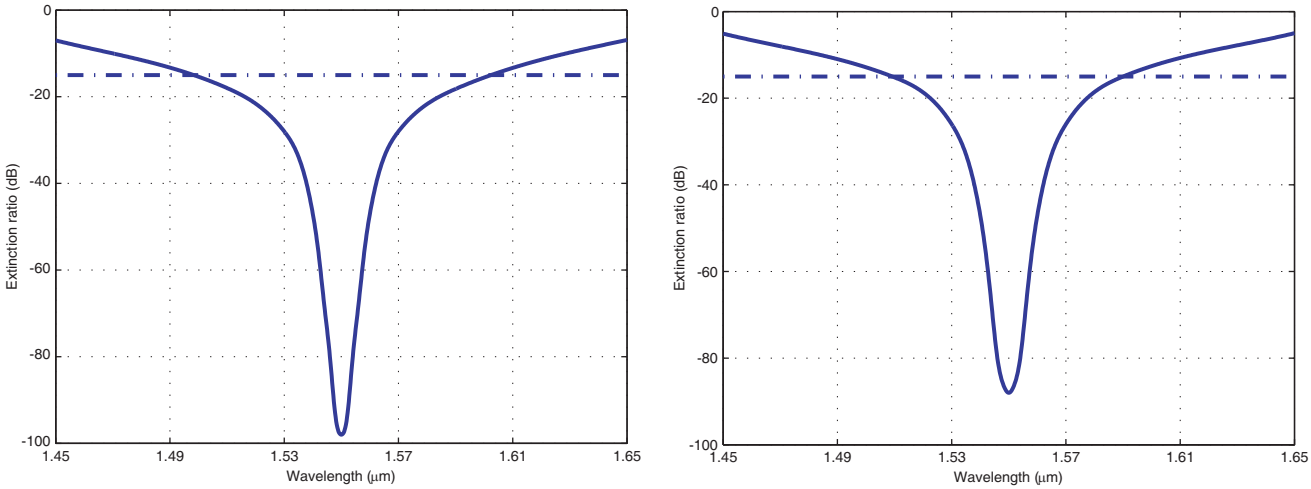

Figure 10. The extinction ratio of the polarization beam splitter versus wavelength for the two optimal structures with lengths of (a) 1.41 mm, and (b) 2.89 mm.

that the extinction ratio can reach 97.7 dB and 88.1 dB at the transmission wavelength of 1.55 μm, and the wavelength bandwidths of extinction ratio better than 15 dB are about 107 and 82 nm, respectively.

4. DISCUSSION AND CONCLUSIONS

To summarize, we have proposed a novel PCF-based PBS with twin highly birefringent cores, and all the air holes are circular holes and are arranged in a triangular lattice that is easy to fabricate with the method of stack and draw. The polarization-dependent coupling characteristics of the proposed splitter are modeled and analyzed by the full-vector FEM and the three-dimensional semi-vector BPM. The simulation results reveal that the polarization dependence of coupling can be significantly enhanced when the birefringence of dual cores is heightened by increasing the diameter of d_1. The analysis of CLR indicates that the eligible CLR values of 3/2 and 4/3 can be obtained when the normalized parameters (d_1/Λ, d_3/Λ) are optimized to be (0.98, 0.32) and (0.88, 0.31) with $\Lambda = 2\,\mu$m, $d/\Lambda = 0.5$ and $d_2/\Lambda = 0.3$. For the two different configurations, the extinction ratio at $\Lambda = 1.55\,\mu$m can reach 97.7 dB and 88.1 dB with different device lengths of 1.41 mm and 2.89 mm, and the wavelength bandwidths of extinction ratio as low as 15 dB are about 107 and 82 nm, respectively.

Compared with the ultra-short PBSs in [28–30], the proposed PCF-based PBS has a larger device length partly resulting from the large distance between the two core centers. However, the larger separation may bring the convenience of connecting with other external devices. In addition, the wavelength bandwidth of high extinction ratio may be further enlarged by introducing depressed-index fluorine-doped cores [25, 26, 36] or embedding a defected air hole into the core in our opinion. Till now, PCFs with different structures have been fabricated by stack-and-draw technique, performs drilling method, die-cast process, and sol-gel casting method, etc. Therefore, the proposed all circular-air-hole PCF-based PBS with the conventional triangular lattice may be fabricated under the current technology. Considering the good performance of the proposed PBS, we believe that it has great potential applications in optical communication systems, such as coherent and polarization diversity optical detection, and the polarization-division multiplexing communication.

ACKNOWLEDGMENT

This work was supported by the National Natural Science Foundation of China under Grant Nos. 51379042, 51379047.

REFERENCES

1. Peng, G., T. Tjugiarto, and P. Chu, "Polarisation beam splitting using twin-elliptic-core optical fibres," *Electron. Lett.*, Vol. 26, No. 10, 682–683, 1990.
2. Hayakawa, T., S. Asakawa, and Y. Kokubun, "ARROW-B type polarization splitter with asymmetric Y-branch fabricated by a self-alignment process," *J. Lightwave Technol.*, Vol. 15, No. 7, 1165–1170, 1997.
3. Wu, C., T. Wu, and H. Chang, "A novel fabrication method for all-fiber, weakly fused, polarization beam splitters," *IEEE Photonic. Tech. L.*, Vol. 7, No. 7, 786–788, 1995.
4. Van der Tol, J. J. G. M., J. W. Pedersen, E. G. Metaal, and Y. S. Oei, "Mode evolution type polarization splitter on InGaAsP/InP," *IEEE Photonic. Tech. L.*, Vol. 5, No. 12, 1412–1414, 1993.
5. Miliou, A. N., R. Srivastava, and R. V. Ramaswamy, "A 1.3 μm directional coupler polarization splitter by ion exchange," *J. Lightwave Technol.*, Vol. 11, No. 2, 220–225, 1993.
6. Bricheno, T. and V. Baker, "All-fibre polarisation splitter/combiner," *Electron. Lett.*, Vol. 21, No. 6, 251–252, 1985.
7. Chen, D, M.-L. V. Tse, and H.-Y. Tam, "Super-lattice structure photonic crystal fiber," *Progress In Electromagnetics Research M*, Vol. 11, 53–64, 2010.
8. Zheng, H. and C. Wu, "Photonic crystal fiber with two triangular arrays of semiminor-axis-decreasing elliptical air holes for single-polarization single-mode operation," *Opt. Eng.*, Vol. 50, No. 12, 125003, 2011.
9. Yin, A. and L. Xiong, "Characteristics analysis of large solid-core square-lattice photonic crystal fibers with hybrid cladding," *Opt. Eng.*, Vol. 53, No. 1, 016112, 2014.
10. Hasana, M. I., M. Selim Habibb, M. Samiul Habibb, and S. M. Abdur Razzakb, "Highly nonlinear and highly birefringent dispersion compensating photonic crystal fiber," *Opt. Fiber Technol.*, Vol. 20, No. 1, 32–38, 2014.
11. Mangan, B. J., J. C. Knight, T. A. Birks, and P. S. J. Russell, "Experimental study of dual-core photonic crystal fibre," *Electron. Lett.*, Vol. 36, No. 16, 1358, 2000.
12. Kakarantzas, G, B. J. Mangan, T. A. Birks, J. C. Knight, and P. S. J. Russell, "Directional coupling in a twin core photonic crystal fiber using heat treatment," *Quantum Electronics and Laser Science Conference*, 7219405, 2001.
13. Lee, B. H., J. B. Eom, J. Kim, D. S. Moon, and U. C. Paek, "Photonic crystal fiber coupler," *Opt. Lett.*, Vol. 27, No. 10, 812–814, 2002.
14. Zhang, L. and C. Yang, "Polarization splitter based on photonic crystal fibers," *Opt. Express*, Vol. 11, No. 9, 1015, 2003.
15. Zhang, L. and C. Yang, "Polarization-dependent coupling in twin-core photonic crystal fibers," *J. Lightwave Technol.*, Vol. 22, No. 5, 1367–1373, 2004.
16. Zhang, L., C. Yang, C. Yu, T. Luo, and A. E. Willner, "PCF-based polarization splitters with simplified structures," *J. Lightwave Technol.*, Vol. 23, No. 11, 3558–3565, 2005.
17. Saitoh, K., Y. Sato, and M. Koshiba, "Coupling characteristics of dual-core photonic crystal fiber couplers," *Opt. Express*, Vol. 11, No. 24, 3188–3195, 2003.
18. Saitoh, K., Y. Sato, and M. Koshiba, "Polarization splitter in three-core photonic crystal fibers," *Opt. Express*, Vol. 12, No. 17, 3940–3946, 2004.
19. Birks, T. A., J. C. Knight, B. J. Mangan, and P. St. J. Russel, "Seeing things in a hole new light-photonic crystal fibers," *Proc. SPIE*, 4532, 206–219, 2001.
20. Mao, D., C. Guan, and L. Yuan, "Polarization splitter based on interference effects in all-solid photonic crystal fibers," *Appl. Optics*, Vol. 49, No. 19, 3748–3752, 2010.
21. Chen, M., B. Sun, Y. Zhang, and X. Fu, "Design of broadband polarization splitter based on partial coupling in square-lattice photonic-crystal fiber," *Appl. Optics*, Vol. 49, No. 16, 3042–3048, 2010.
22. Zhang, L. and C. Yang, "A novel polarization splitter based on the photonic crystal fiber with nonidentical dual cores," *IEEE Photonic. Tech. L.*, Vol. 36, No. 7, 1670–1672, 2004.

23. Rosa, L., F. Poli, M. Foroni, A. Cucinotta, and S. Selleri, "Polarization splitter based on a square-lattice photonic-crystal fiber," *Opt. Lett.*, Vol. 31, No. 4, 441–443, 2006.
24. Florous, N., K. Saitoh, and M. Koshiba, "A novel approach for designing photonic crystal fiber splitters with polarization independent propagation characteristics," *Opt. Express*, Vol. 13, No. 19, 7365–7373, 2005.
25. Lu, W., S. Lou, and X. Wang, "Ultrabroadband polarization splitter based on a modified three-core photonic crystal fiber," *Appl. Optics*, Vol. 52, No. 35, 8494–8500, 2013.
26. Lu, W., S. Lou, X. Wang, L. Wang, and R. Feng, "Ultrabroadband polarization splitter based on three-core photonic crystal fibers," *Appl. Optics*, Vol. 52, No. 3, 449–455, 2013.
27. Jiang, H., E. Wang, J. Zhang, L. Hu, Q. Mao, Q. Li, and K. Xie, "Polarization splitter based on dual-core photonic crystal fiber," *Opt. Express*, Vol. 22, No. 25, 30461–30466, 2014.
28. Liu, Q., S. Li, Z. Fan, W. Zhang, J. Zi, and H. Li, "Numerical analysis of high extinction ratio photonic crystal fiber polarization splitter based on ZnTe glass," *Opt. Fiber Technol.*, Vol. 21, 193–197, 2015.
29. Wang, X., S. Li, H. Chen, G. Wang, and Y. Zhao, "Polarization splitter based on dual-core photonic crystal fiber with octagonal lattice," *Opt. Quant. Electron.*, Vol. 48, No. 4, 271, 2016.
30. Wang, H., X. Yan, S. Li, G. An, and X. Zhang, "Ultra-short polarization beam splitter based on dual core photonic crystal fiber," *J. Mod. Optic.*, Online, 2016.
31. Kim, S. E., B. H. Kim, C. G. Lee, S. Lee, K. Oh, and C. Kee, "Elliptical defected core photonic crystal fiber with high birefringence and negative flattened dispersion," *Opt. Express*, Vol. 20, No. 2, 1385–1391, 2012.
32. Li, J., K. Duan, Y. Wang, X. Cao, Y. Guo, and X. Lin, "Design of a single-polarization single-mode photonic crystal fiber double-core coupler," *Optik*, Vol. 120, 490–496, 2009.
33. Zhang, S., W. Zhang, P. Geng, X. Li, and J. Ruan, "Design of single-polarization wavelength splitter based on photonic crystal fiber," *Appl. Optics*, Vol. 50, No. 36, 490–496, 2011.
34. Saitoh, K. and M. Koshiba, "Numerical modeling of photonic crystal fibers," *J. Lightwave Technol.*, Vol. 23, No. 11, 3580–3590, 2005.
35. Rahman, B. M. A., A. K. M. Saiful Kabir, M. Rajarajan, and K. T. V. Grattan, "Finite element modal solutions of planar photonic crystal fibers with rectangular air-holes," *Opt. Quant. Electron.*, Vol. 37, 171–183, 2005.
36. Laegsgaard, J., O. Bang, and A. Bjarklev, "Photonic crystal fiber design for broadband directional coupling," *Opt. Lett.*, Vol. 29, No. 12, 2473–2475, 2004.